

Effect of Oxygen Adsorption on the Chiral Pt{531} Surface

G. Held,^{*,†} L. B. Jones,^{‡,§} E. A. Seddon,[§] and D. A. King[†]

Department of Chemistry, University of Cambridge, Lensfield Road, Cambridge CB2 1EW, U.K.,
Department of Chemistry, Surface Science Centre, University of Liverpool, Liverpool, U.K., and
CCLRC Daresbury Laboratory, Warrington, U.K.

Received: October 29, 2004; In Final Form: February 8, 2005

The adsorption of oxygen on the chiral Pt{531} surface was studied by high-resolution X-ray photoelectron spectroscopy (HRXPS) and low energy electron diffraction (LEED). After the surface is annealed in oxygen (3×10^{-7} mbar), three O 1s peaks are observed in XPS. One peak, at 529.5 eV, is assigned to chemisorbed oxygen; it disappears after annealing in vacuo to temperatures above 900 K. The other two peaks at 530.8 and 532.3 eV are stable up to at least 1250 K. They are associated with oxide clusters on the surface. These clusters readily react with coadsorbed carbon monoxide at temperatures between 315 and 620 K.

1. Introduction

Certain step-kinked high-Miller-index surfaces of symmetric bulk crystal structures are intrinsically chiral because they have no mirror planes. They are therefore considered as potential templates for enantioselective heterogeneous catalysis where achiral reactants are guided into forming predominantly one enantiomer of a chiral reaction product.^{1–4} There are some examples in the literature of enantioselective reactions on the {531} and {643} surfaces of Pt and Cu.^{2,5–7} Many of these surfaces are, however, not very well characterized by spectroscopic and crystallographic surface science techniques, which makes it difficult to gain insight into the reaction mechanisms at an atomic level.

The present study is part of a series of synchrotron-based experiments, the ultimate goal of which is the study of enantioselective reactions of chiral molecules on Pt{531}. This surface has the smallest two-dimensional unit cell of all chiral Pt surfaces, for which enantioselective reactions have been reported. The small size of the unit cell makes it affordable to employ low energy electron diffraction (LEED) model calculations and *ab initio* calculations based on density functional theory (DFT) in parallel with these experiments. Before enantioselective processes involving complex chiral molecules can be studied in detail, it is necessary to establish the microscopic structure of this rather unusual surface⁸ and to study the basic adsorption properties with respect to small molecular adsorbates such as carbonmonoxide or oxygen.

There is a large database available on the adsorption behavior of CO and oxygen on close packed and some stepped surfaces of Pt (see, e.g., refs 9 and 10 and references therein). As the present study and others show, however, much of the common knowledge acquired from studies of close-packed low-Miller-index surfaces has to be reconsidered, when atomically rough step-kinked surfaces are considered. Among the effects repeatedly reported for oxygen on stepped transition metal surfaces are the formation of double height steps^{11–14} and nanofacet-

ting,^{15,16} which are commonly explained as a means of lowering the total surface free energy of the system.

To our knowledge, oxide formation on Pt single crystal surfaces has so far only been observed under high oxygen pressures in the 1 bar range or above (e.g., see ref 17 and references therein). Subsurface oxygen species, on the other hand, have been observed on several Pt surfaces; they are thought to be precursors to oxide formation (see ref 18 and references therein). This article reports on a Pt–O compound species on Pt{531}, which we identify as Pt-oxide clusters. This, therefore, is the first time that Pt oxide formation is observed under ultrahigh vacuum (UHV) conditions.

2. Experimental Procedures

The experiments were performed at beamline UE52-PGM of the Berlin synchrotron radiation facility BESSYII. A two chamber UHV system with a base pressure in the low 10^{-10} mbar range was used, which is described elsewhere in full detail.¹⁹ The Pt sample was cut from a single-crystal rod, oriented and polished to within 0.5° of the {531}¹⁸ orientation. The chirality of the surface was confirmed by Laue diffraction. For cleaning in vacuo standard techniques were used, including sputtering with Ar ions (500 V; $2 \mu\text{A cm}^{-2}$ for 15 min) and oxygen treatment (2×10^{-7} mbar at 900 K for 15 min) followed by annealing to 1100 K for 5 min.^{15,20,21} The cleaning procedure was completed by 5 cycles of CO adsorption/desorption (see below for further explanation). The temperature (95 K to 1250 K) was monitored by a K-type thermocouple spot-welded to the crystal. High purity carbonmonoxide and oxygen (99.99% from Messer-Griesheim) were admitted through a stainless steel needle doser.

The high-resolution X-ray photoelectron spectroscopy (HRXPS) measurements were performed using linearly polarized synchrotron radiation with photon energies of 650 or 700 eV for O 1s and 650 or 162 eV for Pt 4f spectra. The X-ray spot on the surface was about $90 \times 300 \mu\text{m}^2$. If not noted otherwise, the spectra were recorded at normal emission (incidence angle 55°) using a Scienta 200 mm electron energy analyzer. The binding energy (BE) scale was calibrated with respect to the Fermi edge ($E_F = 0$), which was recorded with the same photon energy and pass energy after each change of the beamline or

* Corresponding author. E-mail: gh10009@cam.ac.uk.

[†] University of Cambridge.

[‡] University of Liverpool.

[§] CCLRC Daresbury Laboratory.

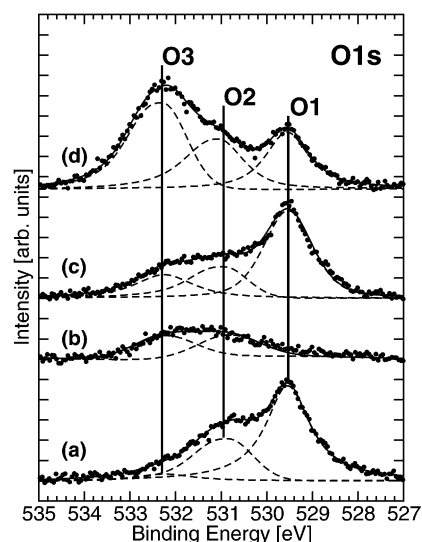


Figure 1. Normal emission O 1s spectra of Pt{531} after (a) annealing at 900 K in oxygen, (b) flashing to 1100 K, and (c) oxygen adsorption at room temperature. (d) was recorded from the same layer as (c) at an emission angle of 55° off the surface normal. Filled circles represent the data points, fitted curves are shown as dashed (single peaks), and solid lines (sum of all peaks); $h\nu = 700$ eV.

analyzer settings. The overall resolution was between 80 meV (162 eV) and 150 meV (700 eV), as determined from the Fermi edge spectra. All intensities were normalized with respect to the background at the low BE side of each spectrum. After a Shirley-type background was subtracted,²² the spectra were deconvoluted using pseudo-Voigt peaks. For the sake of clarity, the fitted peaks are not always included in the figures, however, all peak positions and areas given in the text were determined from the fits.

Because photoelectron diffraction can lead to significant variations in peak intensities for kinetic energies between 90 and 170 eV, as used in this study, larger errors than usual are imposed onto the quantitative analysis of XPS intensities, which is difficult to estimate. By comparing the results from different data sets and different fitting procedures, we estimate the overall error to be around $\pm 10\%$.

3. Results and Discussion

A typical cleaning procedure for low-Miller-index Pt surfaces involves annealing the sample at temperatures of around 900 K in oxygen to remove carbon from the surface by forming gaseous CO or CO₂. On the low index surfaces the remaining chemisorbed oxygen can be removed completely by flashing to 1100 K.^{15,21} If this procedure is applied to Pt{531}, only part of the oxygen desorbs from the surface. Figure 1 shows O 1s spectra for a typical oxygen treatment: (a) after annealing the sample at 900 K for 15 min in an oxygen atmosphere of 3×10^{-7} mbar and cooling to room temperature in oxygen and (b) after annealing to 1100 K for 5 min. Before flashing, a very diffuse superstructure is observed by low energy electron diffraction (LEED), which could not be identified unambiguously but is most likely of the type $(n \times 2)$ ($n \approx 5$). A periodic corrugation compatible with this superstructure was also observed in STM images after a similar treatment.²³ The O 1s spectrum consists of two well resolved peaks at BE 529.5 eV (O1) and 530.9 eV (O2) and a shoulder at 532.3 eV (O3). After flashing to 1100 K, only one broad feature, centered around 531.5 eV, is left and only a $p(1 \times 1)$ pattern is observed by LEED. Spectrum (b) can be fitted with two peaks of about equal

height at BE 530.9 (O2) and 532.3 eV (O3), respectively. This feature persists unchanged even after annealing to 1250 K, which is the highest temperature reached in the experiment. It was also found that the intensity of this feature can vary significantly, by up to a factor of 2, when the sample is scanned with the X-ray beam.

When oxygen is adsorbed at room temperature after this treatment, the O1 peak reappears in addition to the feature in (b) and dominates the spectrum, as shown in (c) of Figure 1. The integrated intensity of the O1 peak in spectrum (c) is 1.3 times the sum of O2 and O3. However, no spots in addition to the (1×1) pattern are observed by LEED. The BE of O1, 529.5 eV, clearly points toward chemisorbed atomic oxygen on the surface, as it is in agreement with BE's found for this species on close-packed Pt surfaces.^{24,25} This chemisorbed oxygen species can be removed completely by annealing to temperatures above 900 K in vacuo, leaving behind only the O2/O3 feature, as in spectrum (b).

Our LEED observations are in general agreement with an earlier study of oxygen adsorption on Pt{210}, which has a nonchiral surface geometry very similar to {531}.¹⁵ On this surface a (5×2) -rect superstructure was only found after adsorbing oxygen at elevated temperatures. Parallel scanning tunneling microscopy (STM) experiments in this study showed that the LEED pattern is due to faceting of the surface. The superstructure disappeared after the main oxygen desorption peak at 700 K. Because no photoelectron-spectroscopic data are reported for this surface, it is not known whether any oxygen species corresponding to O2/O3 is present on this surface after the desorption of chemisorbed oxygen. However, it is clear that on both surfaces the superstructure/faceting is related to a chemisorbed oxygen species desorbing at temperatures well below 1000 K.

The assignment of O2 and O3 is less clear than that of O1. Oxygen-containing molecular adsorbates (e.g., H₂O, OH, CO, O₂ from residual gas) can be excluded as the origin of these features because the annealing temperature is well above their desorption temperatures. Also XPS and Auger peaks due to other contaminants, not containing oxygen, could be excluded. The high BE of the O3 peak and the thermal stability of the corresponding species makes an assignment to chemisorbed atomic oxygen on surface sites very unlikely. But also the most common Pt oxides, PtO and PtO₂, for which the reported O 1s BE's are around 530 (± 1) eV,^{26,27} seem incompatible with O3. An O 1s peak with similar BE was found, however, by Andersen and co-workers for oxygen adsorbed on the stepped Pt{553} surface after annealing in vacuo to temperatures around 1000 K.²⁵ The corresponding oxygen species is stable up to 1400 K.

On Pt{531} similar amounts of CO are found to adsorb at room temperature on both the clean surface and the surface, for which the O2/O3 feature is observed (see below). In addition, the presence of this feature does not significantly affect the desorption properties of CO at low temperatures. It seems that most of the surface area is unaffected by the corresponding oxygen species. This could be explained by this species residing either underneath the topmost Pt layer ("subsurface oxygen") or on the surface as part of small cluster-like islands, which leave a large area of the surface uncovered, able to adsorb CO or additional chemisorbed oxygen. Subsurface oxygen has been associated with high-temperature desorption states around 1000 K on Pt{100}^{20,28} and Pt{110}.^{18,29–31} Under UHV conditions it is usually found only after exposure to excited oxygen molecules or oscillatory reactions of CO and oxygen, none of which was applied in the present case. Also, the O2/O3 species

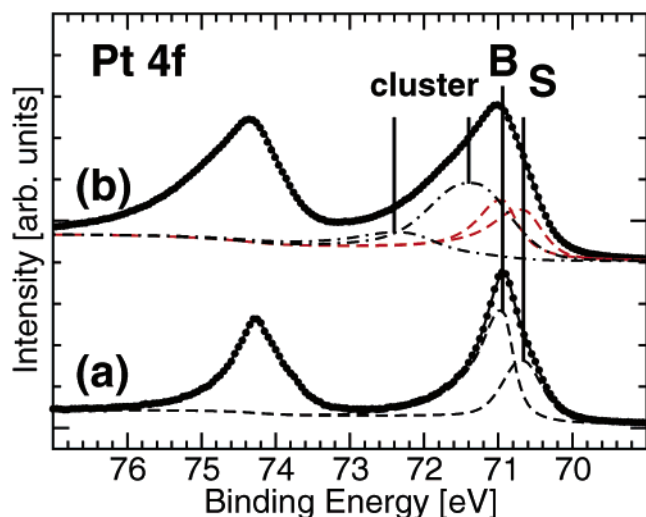


Figure 2. Pt 4f signal for (a) the clean Pt{531} surface and (b) the surface covered with oxide clusters. Filled circles represent the data points, fitted curves are shown as dashed (single peaks) and solid lines (sum of all peaks). For clarity only the peaks fitted to the Pt 4f_{7/2} line are shown. ($h\nu = 162$ eV (a), 650 eV (b); normal emission).

is stable to much higher temperatures than 1000 K. In addition, even though it is not present in the surface layer, subsurface oxygen should still alter the electronic structure and hence the adsorption behavior of the surface significantly. The most striking argument against an assignment to subsurface oxygen is, however, the fact that the relative height of O2 and O3 vs O1 increases dramatically when the spectrum is collected at an emission angle of 55° from the surface normal (spectrum (d)) as compared to the normal emission spectrum for the same preparation conditions (spectrum (c)). This increase is independent of the photon energy and therefore photoelectron diffraction can be excluded as the reason causing this effect. It rather indicates that the oxygen species corresponding to O2/O3 reside indeed at the surface and points toward small clusters. They could be associated with cluster-like features observed in STM images of nominally clean Pt{531} after oxygen treatment.²³ The intensity variations of the O2/O3 feature across the surface could be a consequence of fluctuations in the cluster distribution within the small spot size of $90 \times 300 \mu\text{m}^2$.

The chemical state of these clusters is unclear, however; we can only speculate here. Their high thermal stability suggests that they consist of some kind of Pt oxide; however, as mentioned above, the high O 1s BE's, especially of O3, do not match those reported for the common platinum oxides. If an oxide is formed, one also expects significant shifts in the core levels of the Pt atoms involved. BE shifts of 1.0–1.2 and 2.2–2.9 eV in the Pt 4f levels with respect to the bulk signal of metallic Pt are reported for PtO and PtO₂, respectively.^{26,32,33} Figure 2 shows the Pt 4f_{5/2} and 4f_{7/2} lines for (a) the clean Pt{531} surface and (b) the same surface with the O2/O3 feature but no O1 present. For our discussion we concentrate on the deconvolution of the Pt 4f_{7/2} line because it is better resolved. Both lines were fitted simultaneously, however, to determine the peaks shown in Figure 2. For the clean surface the Pt 4f_{7/2} line shows some intensity centered around BE 70.66 eV (S), in addition to the bulk signal at 70.94 eV (B). S is assigned to surface core level shifts (SCLS) of the low coordinated surface atoms; the shifts are of similar magnitude as the SCLS observed for Pt{111} and stepped vicinal surfaces.^{24,34–36} We refrain from representing each of the four different surface atom coordinations in Pt{531} (6, 8, 10, 11) by a separate peak and use, instead, a relatively broad peak representing the average SCLS

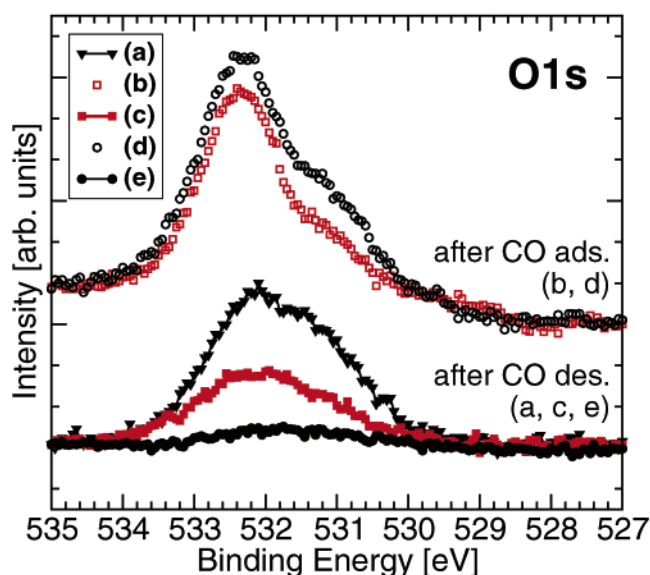


Figure 3. O 1s spectra (a) after oxygen treatment of the Pt{531} surface, (b) after first CO adsorption (45 L at 315 K), (c) after CO desorption (anneal to 620 K), (d) after second CO adsorption (45 L at 315 K), and (e) after second CO desorption (anneal to 620 K). See text for details. ($h\nu = 650$ eV; normal emission).

of all surface atoms. The SCLS feature, S, is still part of spectrum (b) after oxygen treatment. In addition, there is significant broadening of both Pt 4f lines toward higher BE's. This is accounted for by two extra peaks (*cluster*) fitted to the experimental data, which are shifted by 1.3 and 2.3 eV, respectively, with respect to the bulk peak, B. This is much higher than the shift of around 0.7 eV observed for chemisorbed oxygen on Pt{111} and {557}^{24,35} and more in the range of PtO and PtO₂. Because the oxygen-induced shift increases with the O:Pt ratio in these oxides and the peak shifted by 1.3 eV is much larger than the one shifted by 2.3 eV, the O:Pt ratio in the "oxide clusters" is likely to be closer to 1 than 2, possibly similar to the stoichiometry of Pt₃O₄, for which no XPS data exist to our knowledge. It should also be noted that a peak shifted by 1.2 eV, close to the shift of the larger *cluster* peak, was found by Legare et al. after exposing Pt{557} to oxygen under similar conditions.³⁵ On the basis of its increased relative intensity for higher photon energies, the authors assigned this peak to subsurface PtO. For the same arguments the data would, however, also be compatible with oxide clusters on the surface.

The comparison of spectra (a) and (b)/(c) in Figure 1 shows that the intensity of O3 is significantly higher after flashing in vacuo, which is accompanied by oxygen desorption. Therefore, this species must correspond to a more oxygen-depleted environment than O2.

The chemical activity of the O2/O3 oxygen species has been investigated by coadsorbing CO. Figure 3 shows a series of O 1s spectra recorded after consecutive cycles of CO adsorption and desorption. The experiment starts after oxygen treatment with the O2/O3 feature but no chemisorbed oxygen (O1) present at the surface (spectrum (a) in lower part of Figure 3). After the surface is saturated with 45 L CO at 315 K (spectrum (b) in upper part of Figure 3)), an intense peak at BE 532.3 eV, which is due to O3 and additional CO adsorbed on atop sites of Pt{531}, is observed in addition to O2. Annealing the sample to 620 K (c) causes the desorption of CO and leaves behind a much smaller O2/O3 feature than before, which indicates that about half of the O2/O3 species have reacted with CO to form CO₂. After a second adsorption step under the same conditions (d), the peak at BE 532.3 eV is higher in intensity and also the

shoulder at 530.9 eV has grown with respect to spectrum (b), which suggests that some CO also adsorbs on higher coordinated adsorption sites. (Note that a lower O 1s BE usually indicates higher coordinated adsorption sites for CO on transition metal surfaces.^{24,37}) After the second annealing to 620 K (e) almost all oxygen has been removed from the surface. Three to five CO adsorption/desorption cycles were usually enough to remove all oxygen below the detection level of XPS.

This experiment shows that, despite its high thermal stability in vacuo, the O₂/O₃ oxygen species react readily with CO at temperatures between 315 and 620 K. This implies that the oxygen atoms are highly accessible for coadsorbed CO molecules and that their activation barrier for reaction with CO is low. In fact, these "oxide clusters" could be of a nature similar to that of the oxide intermediates observed recently by Hendriksen and Frenken during CO oxidation over Pt{110} at high pressures.¹⁷ For the reasons given above, however, the species described here cannot cover the surface homogeneously as it was found there for the oxide species under high pressure conditions.

The reason similar oxygen species are not observed on close packed Pt surfaces under the same conditions must be connected to the fact that it is easier to create adatoms on high-index surfaces. Pt_xO_y clusters can only be formed when enough mobile Pt adatoms are available at a temperature where oxygen atoms still have a sufficiently long residence time on the surface. The temperature of 900 K, at which the oxygen treatment was performed, is at the upper end of the desorption range of chemisorbed oxygen in UHV.³⁸ A few percent of a monolayer oxygen can be expected to be present at the surface when it is exposed to 3×10^{-7} mbar. The number of Pt adatoms is more difficult to estimate. Comsa et al. have reported the transition from single to double steps at temperatures above 600 K on the stepped Pt{997} surface.¹¹ This implies a large mass transport across the surface, and hence high mobility and a large number of adatoms. On Pt{997} the coordination of step atoms is 7, one less than the coordination of kink atoms on Pt{531}. Assuming a linear relationship between the lowest coordination of surface atoms and activation energy for adatom creation,³⁹ large scale mass transport should be possible on Pt{531} already at about $\frac{6}{7} \times 600$ K = 515 K. Thus, at 900 K plenty of Pt adatoms should be available to form oxide clusters. The diffusion process leading to cluster formation could, however, be more complex and already involve smaller Pt_xO_y clusters similar to the Cu_xS_y clusters that have been identified as the reason for enhanced Cu transport on Cu{111} by Feibelman.⁴⁰ It has also been pointed out that the enhanced adatom diffusion on Pt surfaces in the presence of oxygen may be related to the removal of CO, which blocks diffusion.^{41,42} Because the O₂/O₃ cluster species is formed well above the CO desorption temperature, however, this effect should not play a role here.

4. Summary

After the Pt{531} surface is annealed in oxygen (3×10^{-7} mbar), three peaks are observed in the corresponding O 1s XP spectrum. One peak at BE 529.5 eV is assigned to chemisorbed oxygen; it disappears after annealing to temperatures above 900 K in vacuo. The other two peaks at BE 530.9 and 532.3 eV are thermally stable up to at least 1250 K. Because of their thermal stability and on the basis of chemical shifts in the Pt 4f lines, they are associated with Pt_xO_y oxide clusters on the surface with $x:y$ close to 1. These clusters readily react with coadsorbed carbon monoxide at temperatures between 315 and 620 K.

The presence of such clusters has not been observed before on Pt single crystal surfaces under UHV conditions. They provide a CO oxidation pathway that has previously only been discussed for high-pressure oxidation.

Acknowledgment. This study was supported by the European Commission under the "Human Potential Programme, Transnational Access to Major Research Infrastructures", Contract No HPRI-1999-00028, by a travel grant from the "Verein der Freunde und Förderer von BESSY", by CCLRC and EPSRC. We thank the groups of Profs. Umbach and Freund for lending us their equipment, in particular, Dr. Th. Schmidt and S. Pohl for their support during the measurements, and Dr. S. Pratt for preparing the sample in Cambridge and many helpful discussions. We would also like to thank Prof. J. N. Andersen for helpful discussions and for making his results available prior to publication.

References and Notes

- (1) Sholl, D. S. *Langmuir* **1998**, *14*, 862.
- (2) Attard, G. A. *J. Phys. Chem. B* **2001**, *105*, 3158.
- (3) Gellman, A. J.; Horvath, J. D.; Buelow, M. T. *J. Mol. Catal. A* **2001**, *167*, 3.
- (4) Downs, R. T.; Hazen, R. M. *J. Mol. Catal. A* **2004**, *216*, 273.
- (5) Attard, G. A.; Ahmadi, A.; Feliu, J.; Rodas, A.; Herrero, E.; Blaise, S.; Jerkiewicz, G. *J. Phys. Chem. B* **1999**, *103*, 1381.
- (6) Ahmadi, A.; Attard, G. A.; Feliu, J.; Rodas, A. *Langmuir* **1999**, *15*, 2420.
- (7) Horvath, J. D.; Gellman, A. J. *J. Am. Chem. Soc.* **2001**, *123*, 7953.
- (8) Puisto, S. R.; Held, G.; King, D. A. Submitted for publication.
- (9) Ertl, G. *Surf. Sci.* **1994**, *299/300*, 742.
- (10) Creighan, S. C.; Mukerji, R. J.; Bolina, A. S.; Lewis, D. W.; Brown, W. A. *Catal. Lett.* **2003**, *88*, 39.
- (11) Comsa, G.; Mechttersheimer, G.; Poelsema, B. *Surf. Sci.* **1982**, *119*, 159.
- (12) Koch, R.; Haase, O.; Borbonus, M.; Rieder, K. H. *Surf. Sci.* **1992**, *272*, 17.
- (13) Hoogers, G.; King, D. A. *Surf. Sci.* **1993**, *286*, 306.
- (14) Held, G.; Uremovic, S.; Menzel, D. *Surf. Sci.* **1995**, *331–333*, 1122–1128.
- (15) Sander, M.; Imbihl, R.; Schuster, R.; Barth, J. V.; Ertl, G. *Surf. Sci.* **1992**, *271*, 159.
- (16) Ermanowski, I.; Pelhos, K.; Chen, W.; Quinton, J. S.; Madey, T. E. *Surf. Sci.* **2004**, *549*, 1.
- (17) Hendriksen, B. L. M.; Frenken, J. W. M. *Phys. Rev. Lett.* **2002**, *89*, 046101.
- (18) Walker, A. V.; Klötzer, B.; King, D. A. *J. Chem. Phys.* **2000**, *112*, 8631.
- (19) Wichtendahl, R. Dissertation, Freie Universität Berlin, 1999.
- (20) Guo, X.; Bradley, J. M.; Hopkinson, A.; King, D. A. *Surf. Sci.* **1994**, *310*, 163.
- (21) Mukerji, R. J.; Bolina, A. S.; Brown, W. A. *Surf. Sci.* **2003**, *527*, 198.
- (22) Shirley, D. *Phys. Rev. B* **1972**, *5*, 4709.
- (23) Driver, S. M.; King, M. A. W.; King, D. A. Unpublished results.
- (24) Björneholm, O.; Nilsson, A.; Tillborg, H.; Bennich, P.; Sandell, A.; Hennas, B.; Puglia, C.; Mårtensson, N. *Surf. Sci. Lett.* **1994**, *315*, L983.
- (25) Andersen, J. N., et al. Unpublished results.
- (26) Peuckert, M.; Bonzel, H. P. *Surf. Sci.* **1984**, *145*, 239–259.
- (27) Briggs, D.; Seah, M. P. *Practical Surface Analysis*, 2nd ed.; Wiley: Chichester, 1996; Vol. 1.
- (28) Bradley, J. M.; Guo, X.; Hopkinson, A.; King, D. A. *J. Chem. Phys.* **1996**, *104*, 4286.
- (29) Imbihl, R.; Sander, M.; Ertl, G. *Surf. Sci. Lett.* **1988**, *204*, L701.
- (30) Vishnevskii, L.; Savchenko, V. I. *Kinet. Kalal.* **1987**, *28*, 1516.
- (31) von Oertzen, A.; Mikhailov, A.; Rothermund, H.; Ertl, G. *Surf. Sci.* **1996**, *350*, 259.
- (32) Hecq, M.; Hecq, A.; Delrue, J. P. *J. Less Common Metals* **1979**, *64*, 25.
- (33) Hilaire, L.; Diaz Guerrero, G.; Legare, P.; Maire, G.; Krill, G. *Surf. Sci.* **1984**, *146*, 569–582.
- (34) Apai, G.; Baetzold, R. C.; Jupiter, P. J.; Viescas, A. J.; Lindau, I. *Surf. Sci.* **1983**, *134*, 122–134.
- (35) Legare, P.; Lindauer, G.; Hilaire, L.; Maire, G.; Ehrhardt, J. J.; Jupille, J.; Cassuto, A.; Guillot, C.; Lecante, J. *Surf. Sci.* **1988**, *198*, 69–78.

- (36) Kinne, M.; Fuhrmann, T.; Wheelan, C. M.; Zhu, J. F.; Pantförder, J.; Probst, M.; Held, G.; Denecke, R.; Steinrück, H.-P. *J. Chem. Phys.* **2002**, *117*, 10852.
- (37) Held, G.; Schuler, J.; Sklarek, W.; Steinrück, H.-P. *Surf. Sci.* **1998**, *398*, 154.
- (38) Puisto, S. R. Ph.D. Thesis, Cambridge University, 2004.

- (39) Pimpinelli, A.; Villain, J. *Physics of Crystal Growth*, 1st ed.; Cambridge University Press: Cambridge, 1998.
- (40) Feibelman, P. J. *Phys. Rev. Lett.* **2000**, *85*, 606.
- (41) Esch, S.; Hohage, M.; Michely, T.; Comsa, G. *Phys. Rev. Lett.* **1994**, *72*, 518.
- (42) Feibelman, P. J. *Phys. Rev. Lett.* **1998**, *81*, 168.